TWELFTH EUROPEAN ROTORCRAFT FORUM

Paper no. 37

A QUADRATURE-COLLOCATION TECHNIQUE FOR BOUNDARY ELEMENT METHOD : APPLICATION TO HELICOPTER FUSELAGE

J. Ryan, T.H. Lê

Office National d'Etudes et de Recherches Aérospatiales
BP 72. F - 92322 Châtillon Cedex, France

September 22-25, 1986

Garmisch-Partenkirchen
Federal Republic of Germany

Deutsche Gesellschaft für Luft- und Raumfahrt e. V. (DGLR)
Godesberger Allee 70, D-5300 Bonn 2, F.R.G.

A QUADRATURE-COLLOCATION TECHNIQUE FOR BOUNDARY ELEMENT METHOD : APPLICATION TO HELICOPTER FUSELAGE

J. Ryan, T.H. Lê

Office National d'Etudes et de Recherches Aérospatiales
BP 72. F - 92322 Châtillon Cedex, France

Abstract

This paper is an extension of the authors previous work on a fast collocation boundary method applied to incompressible, inviscid flow. Recent developements are presented and the reliability of this new technique is shown. Comparison of results is shown on a more realistic configuration such as an helicopter fuselage with and without wake.

1. Introduction

Advance in airfoil aerodynamics of high speed helicopters has shown the importance of the fuselage [1-3] and its main aerodynamic characteristic, drag.

A very fast computing code providing velocity and pressure distribution over the whole aerodynamic field with sufficient accuracy is of great use when designing the rotorcraft if only to reduce cost and time in wind tunnel testing.

Over the last few years, ONERA has developed several aspects of the singularity theory such as new methods of resolutions [4], use of independent intersecting meshes [5] and treatment of separated flow [6].

A new boundary collocation method for analysing the incompressible, inviscid flow was developed by Lê-Morchoisne-Ryan [7] with the two main features of speed and low cost, and first applied to simple configurations.

As an extension of this work, this paper presents new calculations on the DFVLR helicopter model [2] and discusses the reliability of this approach.

2. Basic equations and boundary conditions

Consider the three-dimensional, steady, inviscid, irrotational and incompressible fluid flow around an arbitrary body Ω, the perturbation velocity potential $\Phi(\underline{x})$ at any point $\underline{x}$ of the fluid domain Ω' is the solution of problem (P) :

$$(P)\quad \begin{cases} \text{Find } \Phi \in W_o^1(\Omega') = \left\{\Psi \in \mathcal{D}'(\Omega') / \left|\frac{\Psi}{|\underline{x}-\underline{y}|}\right| \in L^2(\Omega'),\ D\,\Psi \in L^2(\Omega')\right\}, \\ \text{such that} \\ \Delta\,\Phi = 0 \text{ in } \Omega' \\ \frac{\partial \Phi}{\partial \underline{n}} = -\,\underline{V}_\infty \cdot \underline{n} \text{ on } \Gamma \end{cases}$$

(see figure 1)

Ω being a bounded open set of R^3,
Γ the boundary of Ω,
Ω' the complementary set of Ω,
$\underline{n}$ the exterior unit normal along Γ,
Γ_W part of the Ω' boundary representing wake surfaces with boundary condition which allows for potential jump, and
$\underline{V}_\infty$ freestream velocity vector.

We shall write :

$\mu\ (\underline{x}) = \Phi|_\Gamma^{int} - \Phi|_\Gamma^{ext}$, for the jump through Γ, of the function defined in R^3.

The perturbation potential is extended by zero in Ω :
$\mu\ (\underline{x}) = - \Phi|_\Gamma^{ext}$.

Using a double layer potential representation [8], the resolution $\Phi\ (\underline{x})$ on Γ can be expressed by :

$$(P_c)\begin{cases} 2\pi\mu\ (\underline{x}) - \int_\Gamma \mu\ (\underline{y})\ \dfrac{\underline{n}_y \cdot (\underline{x} - \underline{y})}{|\underline{x} - \underline{y}|^3}\ ds\ (\underline{y}) = - \int_\Gamma \dfrac{\underline{V}_\infty \cdot \underline{n}_y}{|\underline{x} - \underline{y}|}\ ds\ (\underline{y}) + \\ \qquad \int_{\Gamma_W} \mu_W(\underline{y}) \dfrac{\underline{n}_y \cdot (\underline{x} - \underline{y})}{|\underline{x} - \underline{y}|^3}\ ds\ (\underline{y}) \\ \Phi\ (\underline{x})\ |_\Gamma^{ext} = - \mu\ (\underline{x}) \end{cases}$$

μ_W is the potential jump through Γ_W, and is determined by pressure continuity (Kutta condition).

The velocity vector at any point of Γ is given by :

$$\underline{V}\ (\underline{x}) = - \underline{\nabla}\ \mu\ (\underline{x}) - (\underline{n}_{\underline{x}} \cdot \underline{V}_\infty\ (\underline{x}))\ \underline{n}_{\underline{x}} + \underline{V}_\infty\ (\underline{x})$$

3. Discretisation

The three collocation methods presented here have in common the geometrical panel approximation and compute the flow potential at the panel barycentre $(\underline{x}_i)$ (collocation point).

The body surface Γ and the wake Γ_W are represented by quadrilateral elements (Γ_j) and (Γ_l^W).

Method N° 1, an analytic-collocation method computes all integrals analytically having predefined the behaviour of μ.

Methods N° 2 and 3, quadrature-collocation methods, compute all integrals by quadrature formulae and do not involve any a priori knowledge of the μ behaviour.

3.1. Method N° 1 : the analytic-collocation method
(Hess and Smith Panel Method [9], is used as reference).

μ is set to be constant per panel.
(P_c) becomes :

$$(D_1)\begin{cases} 2\pi\mu(\underline{x}_i) - \sum_j \mu_j \underbrace{\int_{\Gamma_j} \frac{\underline{n}(\underline{y})\cdot(\underline{x}_i - \underline{y})}{|\underline{x}_i - \underline{y}|^3} ds(\underline{y})}_{①} = \\ - \underbrace{\sum_j \int_{\Gamma_j} \frac{\underline{V}_\infty \cdot \underline{n}(\underline{y})}{|\underline{x}_i - \underline{y}|} ds(\underline{y})}_{②} + \underbrace{\sum_l \mu_l^W \int_{\Gamma_l^W} \frac{\underline{n}(\underline{y})\cdot(\underline{x}_i - \underline{y})}{|\underline{x}_i - \underline{y}|^3} ds(\underline{y})}_{③} \end{cases}$$

$\mu_j = \mu(\underline{x}_j)$

$\mu_l^W = \mu(\underline{x}_l^W)$.

Integrals 1, 2, 3 are evaluated analytically.

As these integrals are fairly complex and expensive, they must be computed once and for all and stored on disks.

This is the main inconvenience of this method as these matrices can be quite large.

The matrix thus assembled is then factorized by a L.U. Block algorithm (see [10]).

3.2. Quadrature-collocation methods

3.2.1. Method N° 2 uses a one point quadrature formula, (first studied in [7], the quadrature points being the same as the collocation points.

The general integral $\int_S f(\underline{x}_i, \underline{y})\, ds(\underline{y})$ is approximated by $f(\underline{x}_i, \underline{n}_k)\, w(\underline{x}_k)$, where $w(\underline{x}_k)$ is the weight associated to the quadrature point $\underline{x}_k$. In this paper, $w(\underline{x}_k) = \text{area}(S)$).

When $f(\underline{x}_i, \underline{x}_k)$ is not defined, the singular integral is computed analytically.

(P_c) becomes :

$$(D_2)\begin{cases} 2\pi\mu(\underline{x}_i) - \sum_{j\neq i} \mu(\underline{x}_j) \frac{\underline{n}(\underline{x}j)\cdot(\underline{x}_i - \underline{x}_j)}{|\underline{x}_i - \underline{x}_j|^3} \text{area}(\Gamma_j) \\ = - \sum_j \frac{\underline{V}_\infty \cdot \underline{n}(\underline{x}_j)}{|\underline{x}_i - \underline{x}_j|} \text{area}(\Gamma) + \sum_l \mu^W(\underline{x}_l^W) \frac{\underline{n}(\underline{x}_l^W)\cdot(\underline{x}_i - \underline{x}_l^W)}{|\underline{x}_i - \underline{x}_l^W|^3} \text{area}(\Gamma_l^W) \end{cases}$$

3.2.2. Method N° 3 uses a four point quadrature formula.

An integral such as $\int_\Gamma \mu(\underline{y}) \frac{(\underline{x}_i - \underline{y})\cdot\underline{n}(\underline{y})}{|\underline{x}_i - \underline{y}|^3} ds(\underline{y})$ is approximated by

$\sum_V \mu(\underline{x}_v) \frac{\underline{n}(\underline{x}_v)\cdot(\underline{x}_i - \underline{x}_v)}{|\underline{x}_i - \underline{x}_v|^3} w(\underline{x}_v)$ where

to each $\underline{x}_j$, collocation point, corresponds four $(\underline{x}_v)$, quadrature points, and $w\ (\underline{x}_v)$ are weights associated to points $(\underline{x}_v)$.

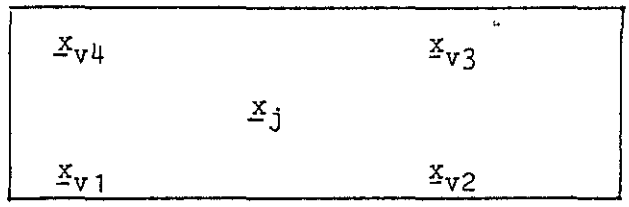

In order to obtain a square matrix, constraints are imposed on the $\mu\ (\underline{x}_v)$.

In this paper, for all $\underline{x}_v$ situated on panel Γ_j with barycentre $\underline{x}_j$, $\mu\ (\underline{x}_v)$ is set to equal $\mu\ (\underline{x}_j)$; $(\underline{x}_v)$ are the panel vertices and $w\ (\underline{x}_v)$ equals 1/4 of area (Γ_j).

(P_c) becomes :

$$(D_3)\begin{cases} 2\pi\mu\ (\underline{x}_i) - \sum\limits_{j\neq i} \mu\ (\underline{x}_j) \sum\limits_{v=1}^{4} \dfrac{\underline{n}\ (\underline{x}_{jv}).(\underline{x}_i - \underline{x}_{jv})}{|\underline{x}_i - \underline{x}_{jv}|^3} \text{ area } (\Gamma_j)/4 \\ = - \sum\limits_{j\neq i} \sum\limits_{v=1}^{4} \dfrac{\underline{V}_\infty \cdot \underline{n}\ (\underline{x}_{jv})}{|\underline{x}_i - \underline{x}_{jv}|} \text{ area } (\Gamma_j)/4 \\ + \sum\limits_{l} \mu^W\ (\underline{x}_l^W) \sum\limits_{v=1}^{4} \dfrac{\underline{n}\ (\underline{x}_{lv}^W).(\underline{x}_i - \underline{x}_{lv}^W)}{|\underline{x}_i - \underline{x}_{lv}^W|^3} \text{ area } (\Gamma_l^W)/4 \end{cases}$$

In the last two methods, the linear systems are solved by means of a steepest descent iterative process and the influence coefficients are computed at each iteration.

This is possible as the calculations are very quick (in both methods, the costs are similar) and therefore saves storing the matrix which is a great advantage over the first method.

The main improvement of the four point over the one point quadrature-collocation method, apart from being more precise, is it avoids the singularity of the panel influence over itself.

4. Numerical results

First results for the quadrature-collocation method with a "one point quadrature" technique have already been presented in ref. [7] in non lifting simple cases.

Comparisons with a four point technique are shown and in order to illustrate the capability of this approach, computations are also performed on the more realistic case of an helicopter fuselage.

4.1. Sphere-non lifting case

An impermeable sphere in a uniform flow was simulated with two networks (512 and 2048 panels).

For this purpose, advantage was taken of one plane of symmetry by paneling only half the sphere, and then calculating the perturbation potential as the sum of the potential induced by the panels and their image.

The three methods described above are evaluated in table 1 by their accuracy and computational cost.

The relative error on velocity in relation to the exact solution is computed in l^2 norm.

Meth. \ Grid	512	2048
1	0.7%	0.3%
2	2.1%	1.4%
3	1.5%	1 %

Relative error

Meth. \ Grid	512	2048
1	5.8s	105s
2	1.1s	10.5s
3	1.5s	12 s

Computing time (CRAY 1S)

Table 1

As can be seen from table 1, computing times have not changed much between methods 2 and 3 though precision has increased by 28%.

In the 2048 panel network, method N° 1 requires 260 000 words and costly I/O procedure while methods N° 2 and 3 only require 180 000 in central memory.

4.2. Helicopter fuselage

The model selected is the DFVLR fuselage configuration (ref. [3]) at angle of attack - 5°.

By taking account of the symmetry, only half the fuselage is discretised with 646 panels and the corresponding half wake with 21 panels (fig. 2).

Method N° 1 took 8.7 seconds, required a memory of 170 000 words while method N° 3 took 2.7 seconds and 110 000 words in central memory.

The wake is modelled by a cylindrical surface parallel to the free stream velocity. A preliminary boundary layer calculation [11] determined the starting line of the wake.

Figure 3 presents a grid view and the location of the wake starting line.

Figure 4 compares results given by the one point and the four point quadrature-collocation methods in the case without wake.

The helicopter nose, meshed by a set of elongated triangles, is better analysed by the four point method which shows a lesser dependence on the meshing idiosyncrasies.

As method N° 3 is more precise and of similar cost, in the following results only methods N° 1 and 3 will be compared.

In figures 5 and 6 are given the pressure distributions along the lower symmetry line of the helicopter fuselage.

Figure 5 compares the measured pressure values with results computed by the classical method (method 1) and those computed by the four point method (method N° 3). Both calculated results are in good agreement up to the precise point at which boundary layer occurs, that is at the aft contraction.

Figure 6 shows a similar comparison, but here the numerical results are computed with wake.

As can be seen, presence of the wake has improved the values in the aft region.

The agreement between experiment and numerical results are fairly satisfying and the quadrature-collocation results (three times cheaper) are close to the analytic-collocation results.

For better agreement, two improvements seem necessary :

- finer meshing of the high gradient zones
- better definition of the wake starting line.

5. Conclusion

- Using a four point instead of a one point collocation method has perceptibly improved the quality of the results while barely increasing the computational costs.

- As a first rendering of lifting cases, set wakes along regular surfaces with a non linear Kutta condition have been added to the non lifting situation, the separation lines having been determined by a preliminary boundary layer calculus.

Results so far are very encouraging :

- A next-step for improving the collocation method will be to consider more accurate quadrature formulae and to search for a good compromise between accuracy and cost.

- This fast technique will make it possible to implant at low cost a wake equilibrium treatment linked to an interactive-boundary layer, inviscid fluid-coupling which will give a better representation of the viscous phenomena.

References

1. A. Cler — Theoretical Analysis of Flow around Helicopter Fuselages : Application to Design and Developments. AGARD Applications of Computational Fluid Dynamics in Aeronautics. 58th Meeting of the Fluid Dynamics Panel Symposium, April 1986.
2. J. Amtsberg, S.R. Ahmed — Wake Characteristics and Aerodynamic Force of a Helicopter Model Fuselage. 9th European Rotorcraft Forum, 1983, Stresa, Italy.
3. J. Amtsberg, G. Polz, A. Vuillet, F. Wilson — Comparison With Experiment of Three Pressure Prediction Method for a Helicopter Fuselage. GARTEUR Helicopter Action Group, March 1984.
4. Y. Morchoisne — Calcul d'écoulements instationnaires par la méthode des tourbillons ponctuels. AGARD Applications of Computational Fluid Dynamics in Aeronautics. 58th Meeting of the Fluid Dynamics Panel. Symposium, April 1986, Aix en Provence. TP ONERA 1986-30.
5. J. Ryan, Y. Morchoisne — Analysis of the Velocity Potential around Intersecting bodies. La Recherche Aérospatiale N° 1986-2, (English edition).
6. T.H. Lê, C. Rehbach — Simulation numérique d'écoulements décollés autour de corps aérodynamiques tronqués. 10th Congrès Canadien de Mécanique Appliquée. June 2-7, 1985, London, Ontario, Canada.
7. T.H. Lê, Y. Morchoisne, J. Ryan — Techniques numériques nouvelles dans les méthodes de singularités pour l'application à des configurations tridimensionelles complexes. AGARD Applications of Computational Fluid Dynamics in Aeronautics. 58th Meeting of the Fluid Dynamics Panel Symposium, Aix en Provence, April 1986.
8. S.G. Mikhlin — Mathematical Physics, an Advanced Course, North-Holland, Amsterdam, 1970.
9. J.L. Hess — Calculation of Potential Flow about Arbitrary Three-dimensional Lifting Bodies. Douglas Aircraft Company AD 699 615, December 1969.
10. H. Boillot, T.H. Lê — Asynchronous I/O Technics and Block Management. First World Congress on Computational Mechanics. The University of Texas, Austin, September 22-26, 1986.
11. C. Gleyzes, J. Cousteix, B. Aupoix — Couches limites tridimensionnelles sur des corps de type fuselage. RT OA N° 4/5025 AYD, 1985 (Unpublished).

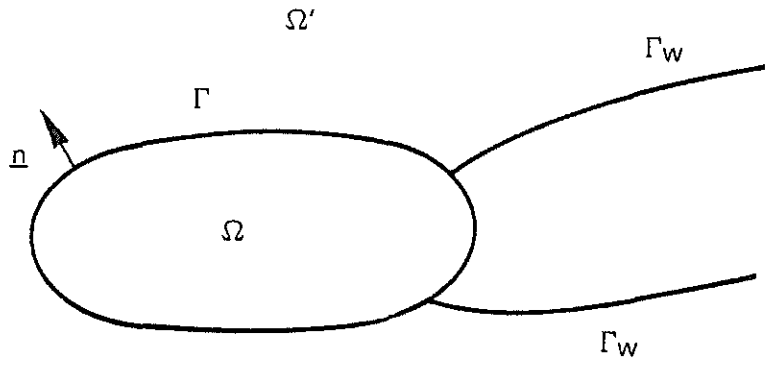

Fig. 1 — Fluid domain and boundaries.

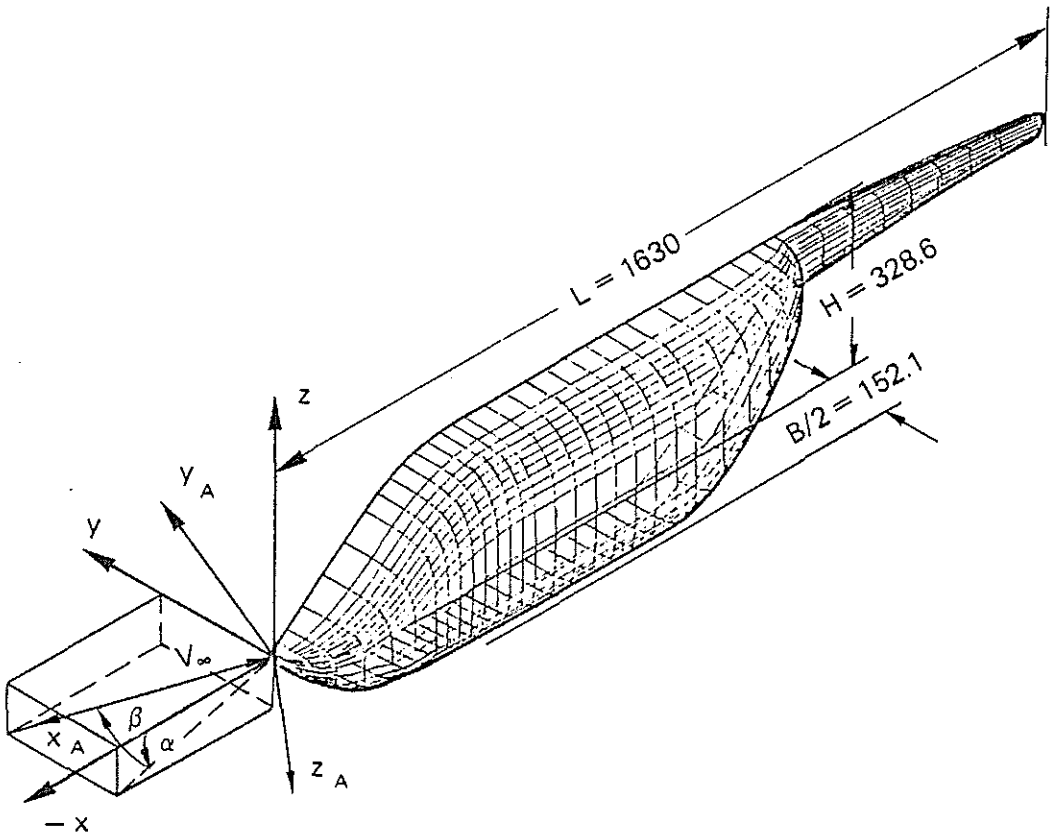

Fig. 2 — Geometry of the helicopter model fuselage.

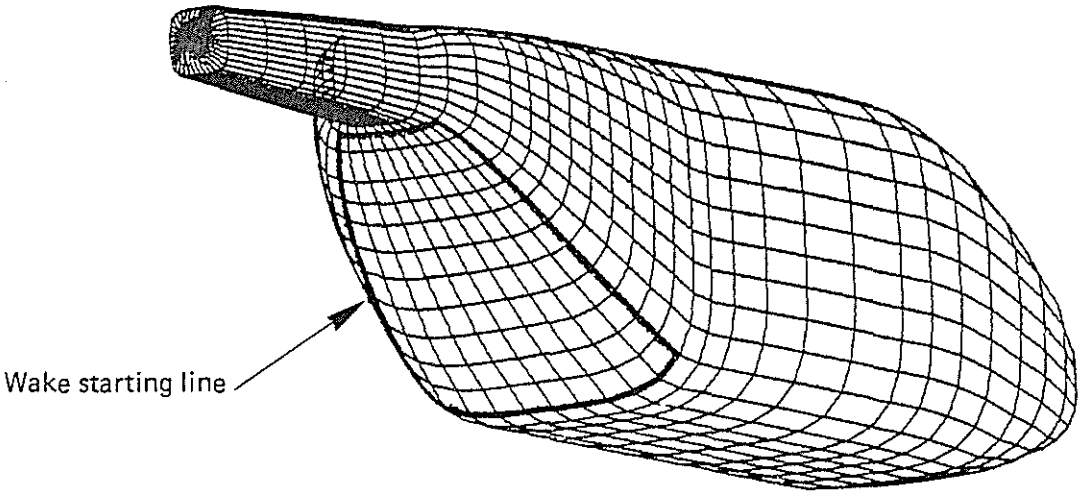

Fig. 3 — Grid view and wake starting line location.

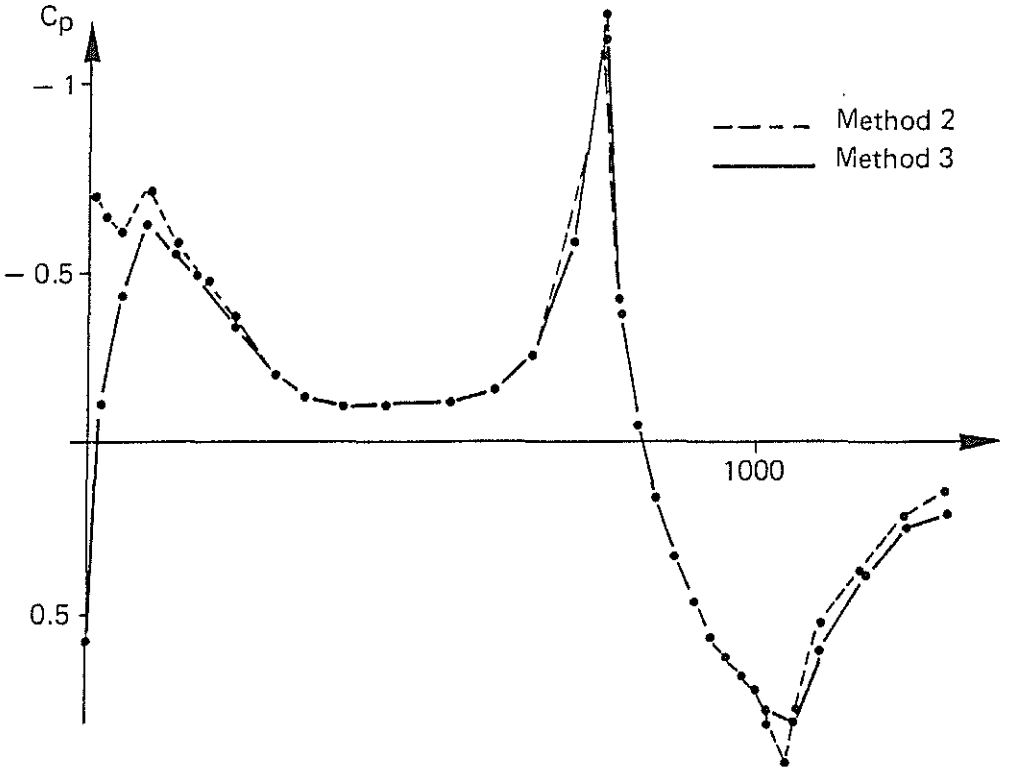

Fig. 4 — Pressure distributions on lower symmetry line without wake.

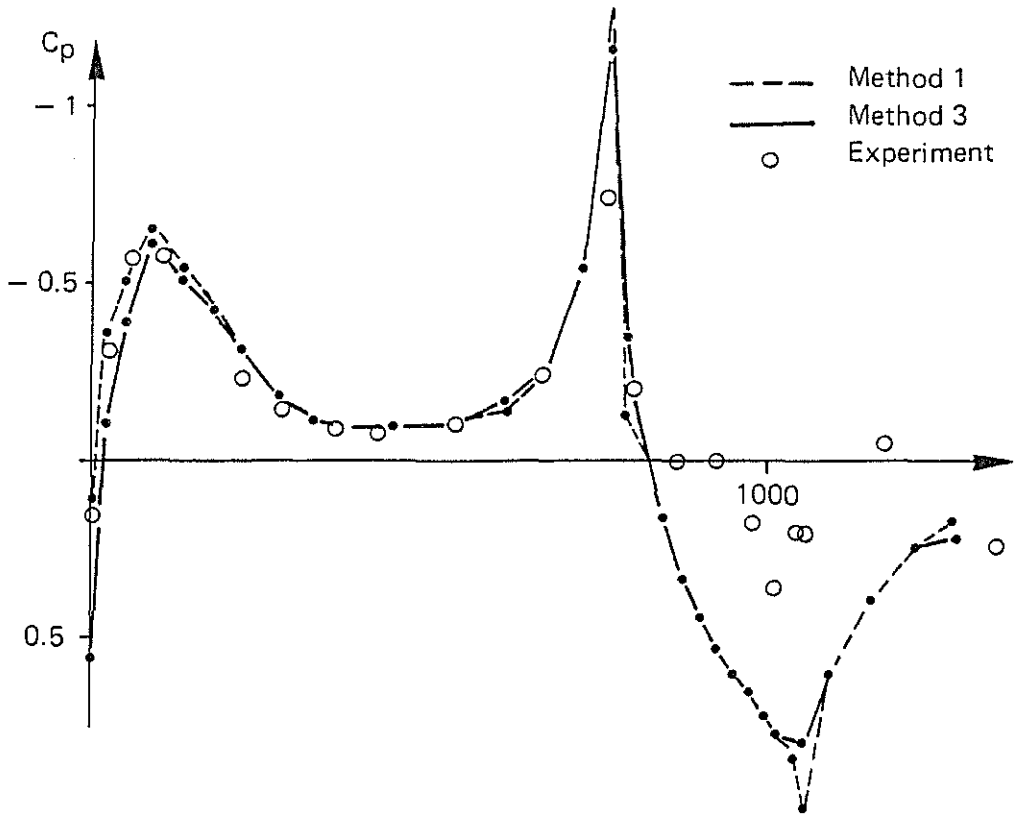

Fig. 5 — Pressure distributions on lower symmetry line without wake.

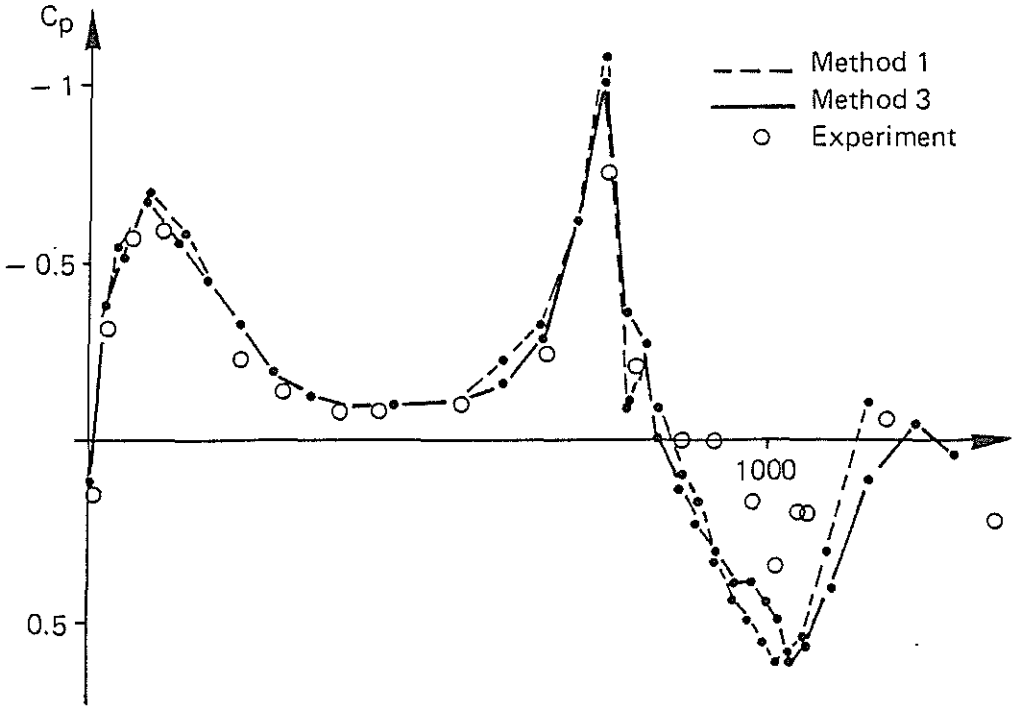

Fig. 6 — Pressure distributions on lower symmetry line with wake.